

ARTICLES

Depth of geological contrast across the West African craton margin

J. C. Briden, D. N. Whitcombe, G. W. Stuart & J. D. Fairhead

Department of Earth Sciences, The University of Leeds, Leeds LS2 9JT, UK

C. Dorbath & L. Dorbath

Office de la Recherche Scientifique et Technique Outre-Mer, 24 Rue Bayard, 75008 Paris, France

Anomalies in teleseismic arrivals at stations astride the West African Craton margin in Senegal are large and systematic for rays which have passed beneath the craton margin. Lateral variation in seismic velocity structure beneath the margin persists to several hundred kilometres depth. The major relative delay time and slowness–azimuth anomalies fit a simple model of a steep boundary in the mantle aligned with the major gravity anomaly associated with the craton margin. The mantle beneath the Mauritanide orogenic belt has lower P-velocity than the adjacent craton between ~80 and 220 km, but higher average velocity both above and below that depth range.

IF mantle structure could simply be categorized as sub-continental and sub-oceanic, there would be no consensus over whether lateral differences persist to depths greater than ~220 km (refs 1–5). Seismological and other evidence indicate a more complex regional characterization of mantle structure. Significant lateral differences occur down to at least 500 km in the vicinity of many active subduction zones^{6,7}. Theory of formation of orogenic belts at convergent plate margins requires the persistence of subduction, and hence of lateral variations to great depths, throughout the period of orogenesis. Surface wave data from Tertiary⁸ and older orogenic belts⁹ suggest that shear wave velocity structure beneath such belts differs from that beneath both ancient cratons and modern oceans. Global and regional teleseismic delay times^{10,11} and heat flow^{12,13} have been taken to indicate lithospheric thicknesses > 200 km in places. Thus differences which arose at the time of orogenesis have persisted for hundreds of millions of years after the cessation of orogenic activity so that determination of present-day seismic structure of ancient orogenic belts may clarify the geodynamics of orogenesis.

We report here preliminary results for temporary teleseismic arrays laid out across the junction of a Precambrian craton with a Phanerozoic orogenic belt to detect lateral differences in mantle seismic velocity structure and to determine whether a boundary between these two regions is detectable to mantle depths.

Location and design of field experiment

Figure 1 shows the site of the experiment in Eastern Senegal, where the western margin of the West African craton (~2,000 Myr and older) abuts the Mauritanide orogenic belt of late Palaeozoic age (~250 Myr).

There are differences of up to 1.0 s in teleseismic delay times between seismic stations on the craton (Kedougou, Fig. 1) and on the orogenic belt¹⁴. The major long-wavelength Bouguer gravity anomaly¹⁵ parallel to the craton margin is characteristic of many craton margins elsewhere^{16,17}. These data suggest that lateral differences across the margin may persist at least into the uppermost mantle.

Two short period vertical (SPz) seismic arrays, each of 20 km aperture, were operated for 6 months: the L-shaped nine station Kedougou (Ked) array on the craton and the cross-shaped eight station Missira (Mis) array centred 180 km to the north-west on the orogenic belt provided travel-time and slowness-data necessary for three-dimensional interpretation of the structure beneath and between them. A mobile linear array of three or four SPz seismometers was placed for 1 month in each of five

successive positions A–E (Fig. 1) to provide records at 10-km spacing along the whole profile between the Ked and Mis arrays. A multichannel analogue tape recorder at the central station of each array recorded an adjacent three component set of short-period seismometers and a single vertical long-period seismometer together with the radio-telemetered signals from the outstations of each array. The internal time base of each recorder was made absolute by recording time signals from BBC World Service transmissions.

All recorded events were digitized at 50 samples per s, and relative arrival times were picked by waveform matching producing overall accuracy of better than 0.05 s. Epicentral

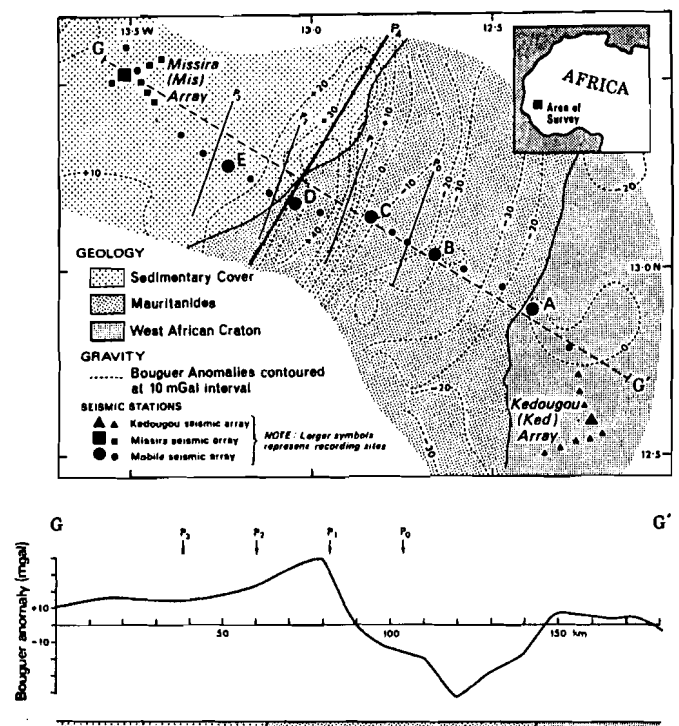


Fig. 1 Part of Senegal, showing the seismic arrays, the Bouguer gravity contours¹⁵, and the Bouguer anomaly profile along the line GG'. P₀ to P₄ are examined positions of a postulated boundary separating cratonic and orogenic velocity structures.

information was taken from USGS PDE bulletins and predicted arrival times were computed utilizing the programme GEDESS¹⁸ with the Jeffreys-Bullen travel-time tables¹⁹. To date 550 seismic events have been identified on the analogue tapes, of which 330 originated in the teleseismic P window, 120 were core phases and the remainder were of local origin. This report considers a subset of the SPz records at the main Ked and Mis arrays, of teleseismic events for which delay times and apparent velocities have been determined, together with some delay time data from the mobile array.

Results

The delay time differences between the central stations of the Mis and Ked arrays are plotted as a function of epicentral distance and azimuth in Fig. 2a. The main features are: rays into the Mis array on the orogenic belt from almost all azimuths and teleseismic distances are slower (positive delays) relative to those into the Ked array on the craton. However, the magnitude of the delays is sensitive to distance and azimuth; between azimuths of $\sim 40^\circ$ and 70° there is a rapid decrease in relative delay time from +0.8 to -0.2 s. The maximum relative delays (+0.8 s) occur for events from the north-east. For westerly azimuths, the delay times decrease with increasing distance from 0.7 s at $\Delta = 60^\circ$ to 0.3 s at $\Delta = 80^\circ$. The relative delays have also been determined for a set of PKIKP core phases in the distance ranges $174^\circ < \Delta < 178^\circ$ and show a similar constant delay of +0.3 s.

Variations of relative delay time along the whole profile are shown in Fig. 3. Each nuclear test site (Fig. 3a-c) can be regarded as a single repeated source. The Kazakh data (Fig.

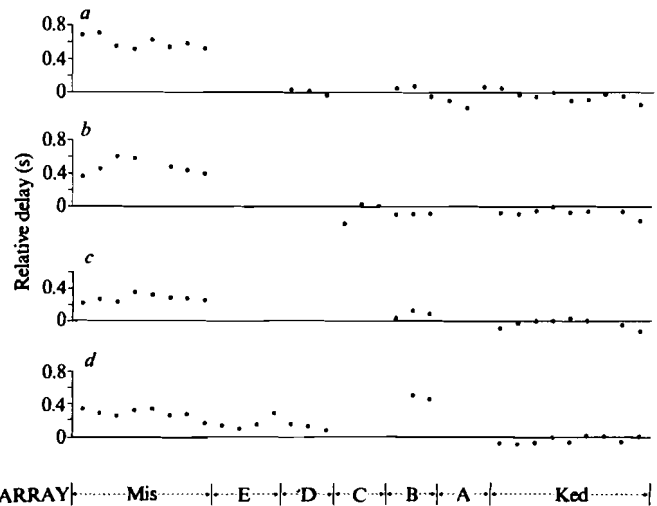


Fig. 3 Teleseismic delay time profiles for underground nuclear tests at a, East Kazakh $\Delta = 80^\circ$, $\phi = 41^\circ$; b, West Kazakh $\Delta = 61^\circ$, $\phi = 42^\circ$; c, Southern Nevada $\Delta = 92^\circ$, $\phi = 309^\circ$; and d for PKIKP phases in the range $174\text{--}178^\circ$.

3a, b) show a sharp westerly increase in relative delay within array E, ~ 80 km west of the outcropping margin. The PKIKP phases (Fig. 3d) have all travelled beneath the receiver structure; they do not show the same pattern of relative delay, though they do show an anomalous (though poorly defined) delay within array B.

Slowness-azimuth anomalies at the Ked array (Fig. 4b) are small and non-systematic from all azimuths except the west; for westerly paths (for rays which have passed beneath the craton-orogenic margin) slownesses are anomalously high and seem to have been refracted across a structure striking NNE. At the Mis array the dominant feature (Fig. 4a) is southerly slowness-azimuth anomalies which are thought to be due to a northerly dipping sedimentary-basement interface.

When the effect of this interface is 'stripped-off' rays from only two sectors appear anomalous (Fig. 4c). Northeasterly arrivals, which have traversed beneath the craton margin, seem to have been perturbed by a NNW-striking structure—slowness being anomalously low for the steepest arrivals but anomalously high for arrivals at larger incidence. Anomalies which persist for azimuths close to 280° could be due to lateral variation in the deep structure of the orogenic belt.

Two-dimensional velocity models

Because the regional strike of the gravity anomaly, the craton margin and the orogenic structure are generally constant and the slowness anomalies follow their local variation, we can treat the seismic data two-dimensionally on a regional scale. In our velocity models we adopt a compromise strike of our models (P_0 - P_3) between the trends of the segments of the line P_4 in Fig. 5.

Models of crustal structure which would produce the observed anomalies all have unacceptable features, notably large lateral velocity contrasts and/or Moho topography which are incompatible with the observed gravity field across the arrays. Hence velocity differences must extend into the upper mantle. The craton has predominantly the higher velocity structure because vertically travelling core phases through the sub-orogenic structure are delayed by 0.3 s. We treat the structure beneath the Mis and Ked arrays as essentially horizontally layered because these arrays are clear of the craton margin and its associated gravity anomaly, and except for ray paths which pass beneath the craton margin, the slowness-azimuth anomaly patterns do not suggest inclined layering at depths²⁰. For such models the azimuth-distance dependence of relative delay times and the drastic change in direction of the slowness-azimuth anomaly vectors for northeasterly arrivals into Mis, both require

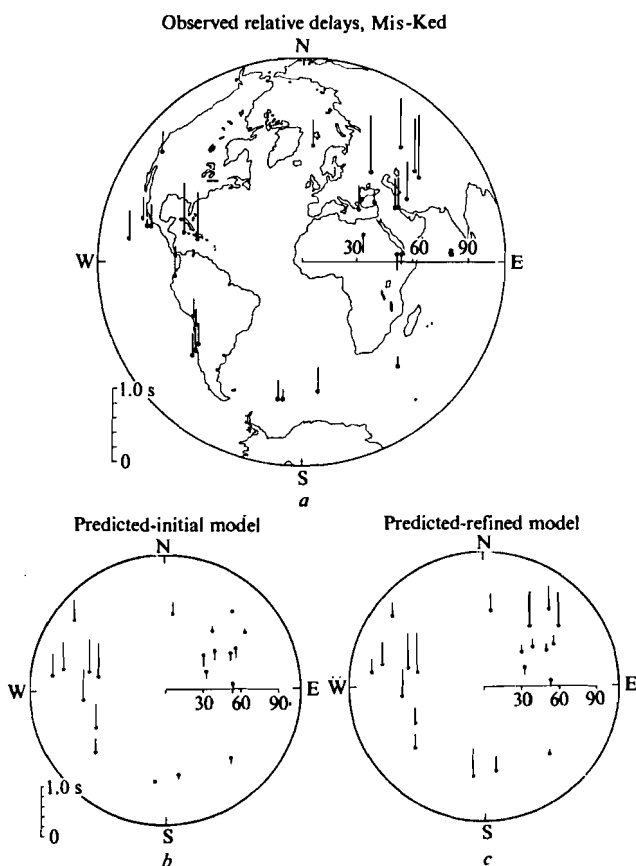


Fig. 2 Teleseismic delay time differences Mis-Ked between the Missira and Kedougou arrays as a function of the position of the source; a, observed; b, predicted by ray tracing through the starting model of Fig. 6a in which the craton boundary is at position P_3 and vertical; c, predicted by ray tracing through the refined model of Fig. 6b in which the craton boundary is at position P_2 and dips at 85° to the west.

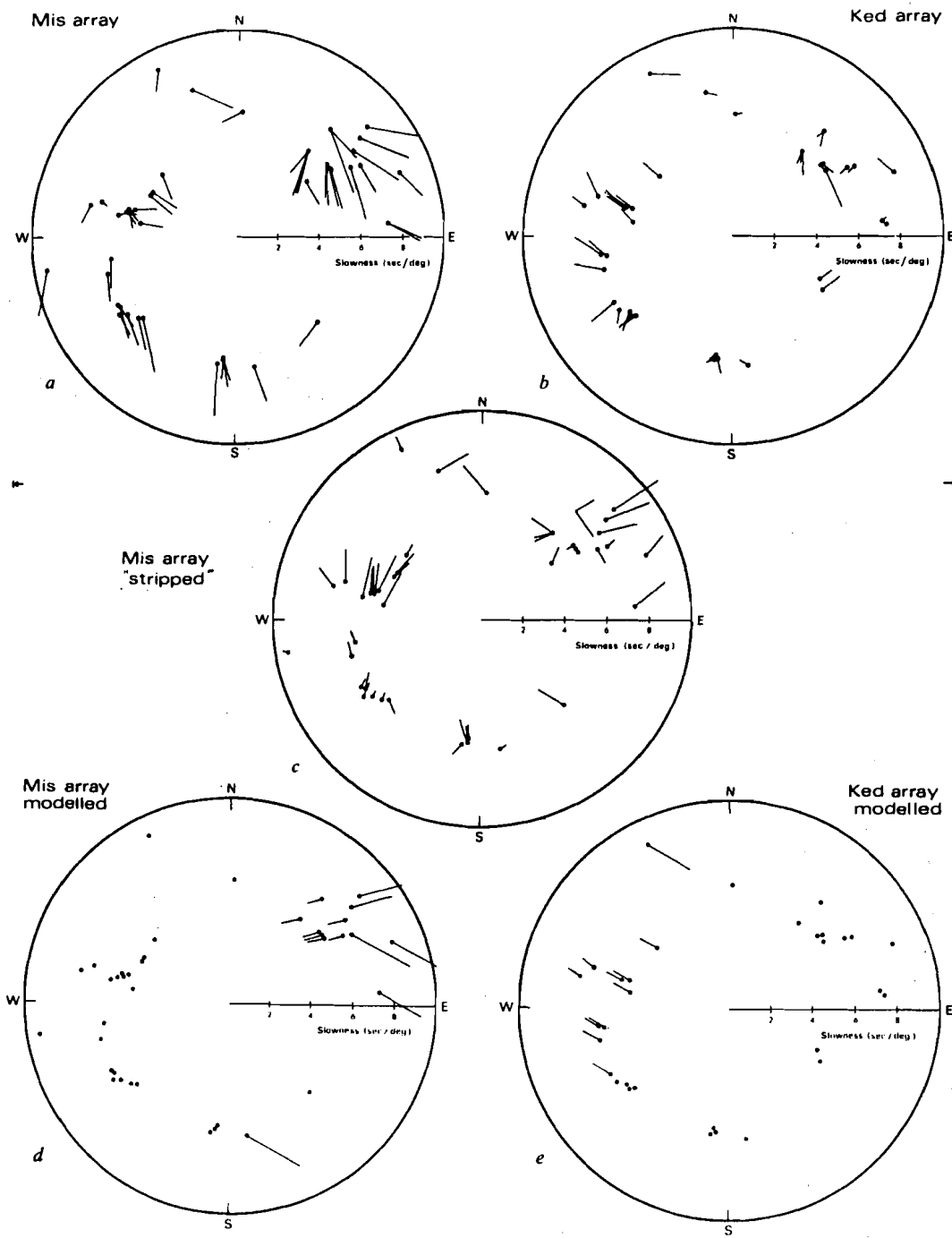


Fig. 4 Slowness anomalies for *a*, Missira; and *b*, Kedougou arrays²⁰. ●, Expected slowness. Anomalies generated at a single interface are orthogonal to the strike of that interface. In *c* the effect of basement topography dipping at 348° azimuth is stripped-off by subtraction of a vector 1.7 s deg⁻¹ in that direction. In *d* and *e* the observations in *c* and *b* are modelled by ray tracing²¹ through the velocity structure of Fig. 6c in the position indicated in Fig. 5.

that between certain depth ranges the orogenic belt has the higher seismic velocity structure. The abrupt change in relative delay times along the profile (Fig. 3) and its marked variation with azimuth (Fig. 2a) require that the transition between the sub-cratonic and sub-orogenic velocity structure is both sharp and steep even at mantle depths.

Two-layer models which account for these anomalous features cannot also account for the negative relative delay times for easterly ray paths (Fig. 2a); these can be accommodated if the orogenic crust is thinner and/or has higher velocity than the cratonic crust. Thus to explain all the main features of the data, we need a model with a minimum of three 'layers' in the crust and upper mantle in which the laterally uniform sub-craton and sub-orogen velocity structures are separated by a near vertical boundary; the top and bottom layers have the higher average velocities beneath the orogenic belt and the middle layer has the higher velocity beneath the craton.

Each layer *i* delays an arrival travelling through the sub-orogenic structure by a time *a_i* relative to an arrival travelling through the same layer in the sub-cratonic structure: thus *a₂* will be positive while *a₁* and *a₃* are negative. Vertically-travelling core phases travel entirely in either sub-orogenic and sub-cratonic velocity structures, so that *a₁* + *a₂* + *a₃* = 0.3 s. The same relative delay terms *a_i* apply to inclined teleseismic paths, errors due to non-verticality being negligible. The relative delays for these inclined paths will depend on the amount of mixing of the rays through the two structures. For example, the high relative delay of +0.8 s from the north-east is interpreted as being due to rays into Mis crossing the model boundary near the bottom of the middle layer: hence *a₁* + *a₂* = 0.8 s. Similarly, negative relative delays for rays from the east which cross the boundary within the top layer, make *a₁* ≈ -0.2 s. Thus *a₂* = 1.0 s and *a₃* = -0.5 s.

If *h_i* is the thickness of the *i*th layer then *a_i* is related to the

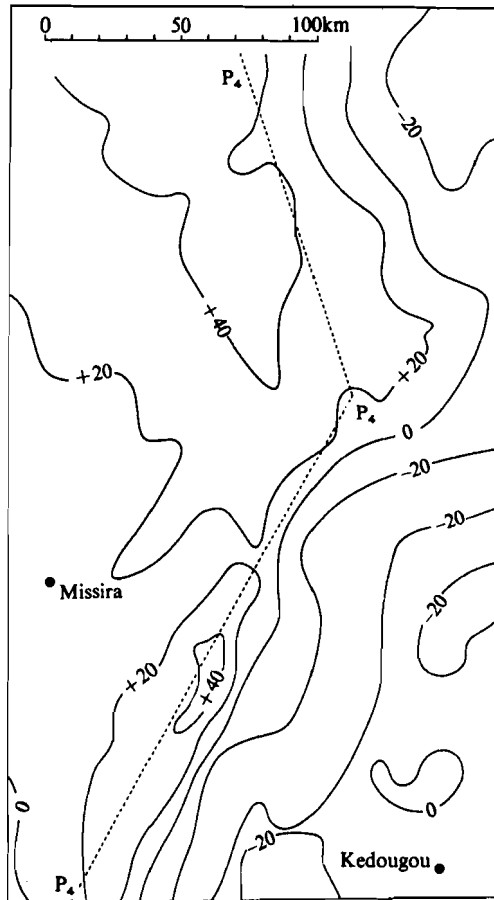


Fig. 5 The position of the seismic boundary P_4 , inferred from the slowness models (Fig. 4d, e) superimposed on the Bouguer anomaly map¹⁵.

average velocities V_{oi} and V_{ci} within that layer beneath the craton and orogen respectively by

$$a_i = h_i \left(\frac{1}{V_{oi}} - \frac{1}{V_{ci}} \right)$$

hence

$$\frac{\delta V_i}{V_i} = \frac{V_i a_i}{h_i}$$

where V_i is the average velocity within layer i and $\delta V_i = V_{ci} - V_{oi}$.

Interpretation of the data requires the thickness of the layers and the position of the boundary to be determined. To satisfy the slowness anomalies and delay time variations from westerly azimuths, rays to Ked from the west must cross the boundary across a negative velocity contrast (within the bottom layer). The largest positive delay times for rays into Mis from easterly azimuths must cross the boundary near the base of layer 2. These two constraints can be met if the boundary at depth occurs west of its outcropping position—a conclusion supported by the nuclear explosion profile data (Fig. 3). More easterly estimates of the position of this boundary lead to contradictory depth estimates for westerly and northeasterly ray-path data. With the boundary at P_3 (Fig. 1) the thickness of the top layer is estimated at 80 km to account for the ray paths which show a relative delay of -0.2 s, assuming that they cross the boundary at the base of layer 1. Arrivals at Ked with anomalously large slowness, cross such a boundary in the depth range 220–390 km while those to Mis with relative delays of 0.8 s cross the boundary at ~ 240 km. Hence the base of layer 2 is taken at 230 km and that of layer 3 at 400 km for our starting model. This definition of model layer thicknesses h_i constrains the velocity

contrasts in each layer to be -1.7% , $+5.4\%$ and -2.8% respectively.

This starting model (Fig. 6a) may now be refined to reconcile all the relative delay time data and to allow for refraction across the boundary, using a 'shooting' ray tracing technique²¹. The fit of predicted and observed delay times for arrivals from the east is further improved by dividing the top layer into two (Fig. 6b). An inadequacy of the starting model is that signals from East Kazakhstan would be internally reflected at the boundary before reaching Mis. This problem would not exist with a lower velocity contrast in the bottom layer, or if the strike of the boundary were bent as in Fig. 5, or if the boundary were inclined at a small angle to the vertical so that it is dipping beneath the orogen. The teleseismic delay times are sensitive to the inclination of the boundary, as rays are travelling steeply through the model. It is difficult to satisfy the large relative delays from the north-east with the smaller relative delays from the west unless the dip of the boundary deviates from the vertical. The refined model (Fig. 6b), which has the surface expression of the boundary at P_2 , and the dip of the contact as 85° towards the west, displays the main features of the observed relative delay time pattern: compare Fig. 2c with Fig. 2a.

To investigate further the interdependence of model parameters, the relative delay times have been directly inverted by a modification of the least squares technique of Aki *et al.*²². This modification divides each layer of the model into two to simulate sub-cratonic and sub-orogenic structure. The block boundary, which need not be vertical, thus simulates the actual lateral velocity discontinuity within each layer. The travel time of each ray through each block is calculated using three-dimensional ray tracing²¹. This inversion method mimics the tectonic regionalizations common for surface wave dispersion studies²³. The trial models allowed for velocity differences down to 400 km, either side of a vertical or near vertical boundary in positions P_0 , P_1 , P_2 and P_3 (Fig. 1).

The lowest solution variance occurred with the boundary at a position P_2 , and dipping beneath the orogenic belt between 85° and 80° . This solution accommodated $\sim 80\%$ of the observed data variance. Ray tracing through this inversion model yields predicted delay times similar to those of Fig. 2c. The most consistent feature of all the solutions with variance close to the minimum is the region in which the sub-cratonic structure has the higher velocity: this occurs at a depth 80–200 km if the boundary is at the preferred position P_2 consistent with the

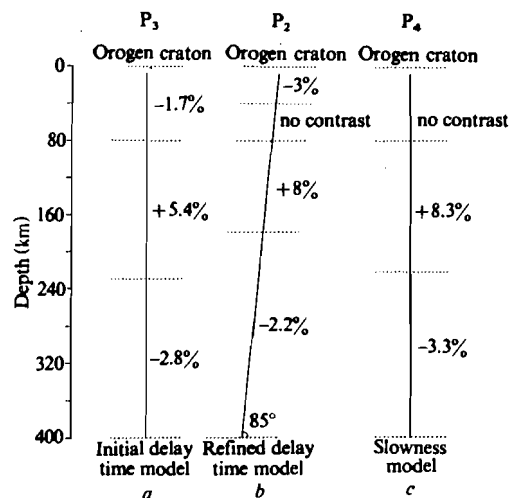


Fig. 6 Velocity contrast models obtained by forward modelling using three-dimensional ray tracing. For all these models the boundary between the craton and orogenic velocity structure is assumed to be planar and positioned at P_2 , P_3 or P_4 (see Fig. 1). The dip of the boundary is represented to true scale. The contrasts in the slowness model c must be greater to explain the magnitude of the observed slowness anomalies in Fig. 4.

deductions from forward ray tracing. If the boundary were only 20 km to the east (P_1) the equivalent layer would be displaced downwards by 40 km; a comparable upward displacement of this layer would be inferred if the boundary lay 20 km to the west (P_3).

All solutions tend to show higher average velocities beneath the orogenic belt below this layer down to 400 km (layer 3 in the ray tracing modelling). However, neither this 'layer' nor the detailed velocity structure within it is well defined, probably because the velocity perturbations are small and comparable with their standard errors.

Although the inversions do not define a top layer as clearly as the ray tracing approach they do suggest a faster velocity structure within the top 80 km beneath the orogenic belt as inferred from ray tracings. The velocity perturbations determined by the inversions are all smaller than the equivalent velocity perturbations obtained by ray tracing. Simulated data studies²⁸ have demonstrated that this inversion method can underestimate the magnitude of velocity anomalies.

Aspects of three-dimensional modelling

The slowness–azimuth anomaly patterns (Fig. 4*b, c*) require that their causative structure should not be precisely linear. A seismic boundary positioned along the line P_4 in Fig. 5 gives a 'best' fit to the data in conjunction with the velocity contrast model in Fig. 6*c* in that it reproduces the magnitude and direction of the slowness anomalies for westerly paths into Kedougou and the antiparallel slowness anomaly for the NNW event (Fig. 4*e*) and reproduces the size, orientation and (to some extent) azimuth dependence of the slowness anomalies from the north-east quadrant into Missira (Fig. 4*d*). Because the line P_4 was chosen on the basis of the seismic data, the concordance of its strike with that of the Bouguer anomaly (Fig. 5) is noteworthy. (The coincidence of its position in Fig. 5 is of less significance because position and dip of the model boundary and depths of the layers are to some extent mutually traded-off in the search for acceptable models.)

Although the teleseismic P and PKIKP data recorded by the end-arrays are fitted well by the models, the isolated observation of large relative delays for a PKIKP event recorded within subarray B (Fig. 3*d*) is not predicted, and the more complex model required must await more data, notably from the mobile array.

Tectonic interpretation of the seismic models

The contrast in background Bouguer anomaly between the craton and the orogenic belt (Fig. 1) is consistent with the cratonic crust being either thicker or having lower average density (and seismic velocity) than the orogenic crust, and hence is consistent with the uppermost part of the seismic model (Fig. 6).

The seismically-determined craton margin at depth lies ~80 km west of the outcropping margin, implying at least that amount of thrusting and/or depositional overlap of the rocks of the orogenic belt onto the craton. This intervening terrain is composed of a metamorphic belt (correlating with the linear positive Bouguer anomaly) and a zone of unmetamorphosed sediments and volcanics (correlating with the negative Bouguer anomaly, and pinching out with it in the north of Senegal); these correlations suggest that the causes of the linear Bouguer anomalies are within the overlap–overthrust rocks of the upper crust.

The major seismic velocity contrasts along the profile occur within the depth range ~80–200 km where the sub-cratonic structure is the faster by ~6%. This result is consistent with delay time inversion studies of lateral differences between older and younger orogenic regions in North America^{3,24} and in Europe²⁵ with the older structures having the higher velocities. The depth range 80–200 km also correlates well with the S-wave low velocity zone determined by the inversion of surface waves beneath aseismic continents²⁶. We thus prefer to ascribe the 6% P velocity contrast to a low velocity sub-orogenic

structure rather than to an anomalously high velocity sub-cratonic structure.

At depths ≥ 200 km the younger, sub-orogenic, structure has the higher velocity, although the contrast is not as marked (~3%). It may be argued that such a small contrast may be a random fluctuation in velocity, and not correlatable with the tectonics. However, studies in North America and Europe^{3,24,25} have revealed similar features: cratonic North America has 2–3% lower velocity in the depth range 250–400 km than both the Appalachians and Western Cordillera. Similarly the Precambrian Grenville Province has lower velocities than the Palaeozoic Appalachian Province for the depth range 200–350 km (ref. 24). Within Europe in the depth range 250–400 km the P-wave velocity beneath the Alps is up to 2% higher than beneath adjacent areas²⁵. Furthermore the interpretation of NORSAR travel-time data using the Herglotz–Wiechert inversion technique indicates that the Baltic craton has higher velocities than orogenic Europe down to 300 km, while in the depth range 300–420 km it has the lower velocities²⁷.

Because of the difficulties²⁹ of determining the depth of origin of teleseismic travel time anomalies, it is worth emphasizing that the principal grounds of our identification of deep lateral variations are: (1) the large epicentral dependence of relative delay times of ~1.0 s require lateral variations in upper mantle structure; (2) slowness anomaly vectors orthogonal to the local strike of the long wavelength gravity anomaly and craton margin imply that the seismic anomalies are inherently associated with that margin. Furthermore a reversal of the anomaly vectors at each array provides direct evidence for a velocity contrast reversal with depth. Such a model will accurately predict the major delay time anomalies.

If density contrasts at depth alternate then isostatic compensation depths may be much deeper (~400 km) than hitherto suspected. The gravity anomaly observed at surface may be regarded as the sum of several individual anomalies of alternate sign, generated in alternate depth zones: because these contributions will partially cancel each other out, the observed anomaly will not fully reflect the magnitude and extent of sub-surface contrasts. Relative teleseismic delay times for vertical paths to cratonic and orogenic stations show a similar effect if the boundary is near vertical: if we had taken delay times for vertical paths only or calculated a mean delay time for each station we would have inferred much less contrast and our models would not have extended to such great depths. It is the larger differential delay times from inclined ray paths which allow this deeper structure to be recognized.

It is beyond the scope of this article to speculate on the possible origin of a mantle boundary such as that inferred here, extending essentially vertically to 400 km into the mantle, but some preliminary points are worth noting. For example, where the lithospheric thickness exceeds ~300 km most sources of continental magmatism must be travelling with the lithospheric plate and must evolve with time, with or without replenishing mechanisms. If lithospheric thickness is variable, then the asthenosphere has considerable topography and variable thickness which would act as controls on plate motion. The near vertical attitude of a boundary within the upper mantle is not obviously compatible with an origin either at a compressional plate margin or an extensional margin; explanations may have to be sought in relation to transcurrent tectonics³⁰ (as has been suggested for the north-west margin of the West African craton on palaeomagnetic grounds³¹) or ideas about the deep thermal structure of plate margins may need revising.

This research has been funded by the Natural Environment Research Council, and Office de la Recherche Scientifique et Technique Outre-Mer. We thank ORSTOM, the Institute of Geological Sciences Edinburgh, and MOD(PE) Blacknest for assistance. IPG Contribution No. 513.

Received 4 February; accepted 14 May 1981.

- Jordan, T. H. *Rev. Geophys.* **13**, 1 (1975).
- Powell, C. *Nature* **254**, 40 (1975).
- Romanowicz, B. A. *Geophys. J. R. astr. Soc.* **57**, 479 (1979).

4. Anderson, D. L. *J. geophys. Res.* **84**, 7555 (1979).
5. Okal, E. A. & Anderson, D. L. *Geophys. Res. Lett.* **2**, 313 (1975).
6. Engdahl, E. R. *Geophys. Res. Lett.* **2**, 420 (1975).
7. Jordan, T. H. *J. Geophys.* **43**, 473 (1977).
8. Menke, W. H. *Bull. seism. Soc. Am.* **67**, 725 (1977).
9. Haddon, R. A. W. & Husebye, E. S. *Geophys. J. R. astr. Soc.* **55**, 19 (1978).
10. Sengupta, M. K. & Julian, B. R. *Bull. seism. Soc. Am.* **66**, 1555 (1976).
11. Fairhead, J. D. & Reeves, C. V. *Earth planet. Sci. Lett.* **36**, 63 (1977).
12. Pollack, H. N. & Chapman, D. S. *Tectonophysics* **38**, 279 (1977).
13. Gaas, I. G., Chapman, D. S., Pollack, H. N. & Thorpe, R. S. *Phil. Trans. R. Soc. A288*, 581 (1978).
14. Dorbath, C. & Dorbath, L. *Cah. Géophys. ORSTOM* No. 16, 27 (1979).
15. Crenn, Y. & Rechenmann, J. *Cah. Géophys. ORSTOM* No. 6 (1965).
16. Gibbs, R. A. *Earth planet. Sci. Lett.* **27**, 378 (1975).
17. Mathur, S. P. *Tectonophysics* **24**, 151 (1974).
18. Young, J. B. & Gibbs, P. G. *AWRE Rep. No. 0 54/68* (HMSO, London, 1968).
19. Jeffreys, H. & Bullen, K. E. *Gray Milne Trust* (reprinted by Smith & Ritchie, Edinburgh, 1967).
20. Briden, J. C., Mereu, R. F. & Whitcombe, D. N. *Geophys. J. R. astr. Soc.* (submitted).
21. Whitcombe, D. N. *Geophys. J. R. astr. Soc.* (submitted).
22. Aki, K., Christofferson, A. & Husebye, E. S. *J. geophys. Res.* **82**, 277 (1977).
23. Lévêque, J. J. *Geophys. J. R. astr. Soc.* **63**, 23 (1980).
24. Taylor, S. R. & Toksöz, M. N. *J. Geophys. Res.* **84**, 7627 (1979).
25. Romanowicz, B. A. *Geophys. J. R. astr. Soc.* **63**, 217 (1980).
26. Knopoff, L. *Tectonophysics* **13**, 497 (1972).
27. England, P. C., Worthington, M. H. & King, D. W. *Geophys. J. R. astr. Soc.* **48**, 71 (1977).
28. Smith, M. L., Julian, B. R., Engdahl, E. R., Gubbins, D. & Gross, R. *EOS* **59**, 1130 (1978).
29. Christofferson, A. & Husebye, E. S. *J. geophys. Res.* **84**, 6168 (1979).
30. Sutton, J. & Watson, J. V. *Nature* **274**, 433 (1974).
31. Onsott, T. C. & Hargraves, R. B. *Nature* **289**, 131 (1981).

Purified λ regulatory protein *cII* positively activates promoters for lysogenic development

Hiroyuki Shimatake & Martin Rosenberg

Laboratory of Biochemistry, National Cancer Institute, National Institutes of Health, Bethesda, Maryland 20205, USA

The bacteriophage λ regulatory protein, cII, has been purified and shown to activate positively RNA transcription from the two phage promoters which coordinately regulate phage lysogenic development. To obtain this protein, the cII gene was cloned into a plasmid vector carrying the strong, regulatable λ phage promoter P_L such that it was overproduced to levels approaching 5% of cellular protein.

WHEN bacteriophage λ infects *Escherichia coli* cells, the phage can either grow lytically, resulting in the formation of new progeny virus particles which are released on lysis of the host cell, or the phage may enter a state of lysogeny, in which the viral DNA integrates into the host genome and the expression of lytic functions is repressed. In normal physiological conditions, a balance between lytic and lysogenic growth is achieved and appreciable numbers of cells enter both developmental pathways¹⁻⁴.

The establishment of the lysogenic state requires the synthesis of two phage functions—repressor (*cI*), a protein which inhibits transcription of lytic functions, and integrase (*int*), a protein which catalyses the integrative recombination between the viral DNA and the host genome. The production of both proteins is positively regulated by the phage gene products *cII* and *cIII* and also affected by various host-encoded functions^{5,6}. The synthesis of repressor and integrase is coordinately controlled at the level of transcription from the two λ promoters P_E and P_I (Fig. 1). The DNA structure of these two sites has been determined⁷⁻¹⁰ and their location precisely defined^{11,12}. Little is known, however, about the precise roles of the *cII* and *cIII* gene products in this activation process. In particular, it is not known whether *cII* works alone or in combination with other factors or whether *cII* works directly or indirectly to activate transcription from P_E and P_I . Only by purifying the components and reconstituting the positive activation system *in vitro* can we hope to elucidate the role of *cII* and understand positive activation at these two promoters.

Cloning a 'lethal' gene function

During a normal λ infection, *cII* protein is synthesized for only a short time and seems to be rapidly turned-over¹³. Thus we set out to clone the λ *cII* gene into a plasmid vector in such a way that the gene would be efficiently and continually expressed. The general approach involved inserting a 1,300-base pair (bp) DNA fragment carrying the *cII* gene into a plasmid vector, in such a way that the *cII* coding region was positioned in proper orientation downstream from an efficient promoter signal for RNA transcription. We reasoned that efficient transcriptional expression of *cII* from the multicopy vector would result in high-level *cII* production. The purified 1,300-bp DNA fragment^{7,14} was inserted into several different derivatives of pBR322, each of which contained a known promoter signal of

either phage or bacterial origin positioned upstream from the site of insertion. Recombinants (Amp^r) were screened by size and restriction analysis for the presence of the fragment. Among multiple independent isolates (>10) which contained the insert, all had the fragment positioned with the *cII* coding region in opposite orientation to the direction of transcription. It appeared that transcriptional expression of the fragment gave rise to some lethal function.

This contention was supported by the facts that cleavage of the fragment at the single *HincII* restriction site within the *cII* gene now allowed each subfragment to be cloned downstream from the promoter signal, and that the entire fragment was readily inserted in both orientations into a pBR322 derivative lacking the promoter.

To circumvent these problems we reasoned that the *cII* gene (as well as any other lethal function) would have to be cloned such that its expression could be regulated. Thus we utilized a pBR322 derivative, pKC30, which contained a λ DNA fragment carrying the highly efficient promoter signal P_L (Fig. 1). This promoter can be regulated by the λ repressor protein (*cI*), a product which is synthesized continually and is regulated auto-genously in an *E. coli* λ lysogen¹⁵. A *HpaI* restriction site unique to pKC30 (Fig. 1) is located 321bp downstream from the start site of P_L transcription. The 1,300-bp DNA fragment carrying the *cII* gene was inserted into this site and transformants (Amp^r) were selected in an *E. coli* λ lysogen. In contrast to our initial results, recombinants were now obtained carrying the intact 1,300-bp DNA fragment positioned in both possible orientations relative to P_L -directed transcription. The desired recombinant, pKC30*cII*, carries the *cII* gene oriented correctly with respect to P_L transcription, whereas the recombinant pKC30*IIc* carries the same fragment inserted in reverse orientation. When these plasmids were used to retransform both lysogenic and non-lysogenic *E. coli* strains, pKC30*IIc* transformed both strains with high efficiency, whereas pKC30*cII* only transformed the lysogen with high efficiency and was unable to transform the non-lysogen. Apparently, the amount of repressor being synthesized in the single lysogen is sufficient to reduce *cII* expression in the pKC30*cII* derivative to a non-lethal level.

To express the *cII* gene product in the lysogen, it was necessary to induce (derepress) the P_L promoter, by using a lysogen which carried a temperature-sensitive mutation in the phage repressor gene (*cI857*)¹⁶. Thus, raising the temperature of these